https://doi.org/10.5194/acp-2019-444
Preprint. Discussion started: 12 June 2019

Atmospheric Chemistry and Physics Discussions

Spatiotemporal variation of aerosol and potential long-range transport impact over Tibetan Plateau, China

Jun Zhu[1,2,3], Xiangao Xia[2,4], Huizheng Che[3], Jun Wang[5], Zhiyuan Cong[6], Tianliang Zhao[1], Shichang Kang[7,9], Xuelei Zhang[8], Xingna Yu[1], Yanlin Zhang[1]

[1] Collaborative Innovation Center on Forecast and Evaluation of Meteorological Disasters, Key Laboratory for Aerosol-Cloud-Precipitation of China Meteorological Administration, Nanjing University of Information Science and Technology, Nanjing 210044, China;
[2] LAGEO, Institute of Atmospheric Physics, Chinese Academy of Sciences, Beijing 100029, China;
[3] State Key Laboratory of Severe Weather (LASW) and Key Laboratory of Atmospheric Chemistry (LAC), Chinese Academy of Meteorological Sciences, CMA, Beijing, 100081, China;
[4] University of Chinese Academy of Sciences, Beijing, 100049, China;
[5] Center of Global and Regional Environmental Research and Department of Chemical and Biochemical Engineering, University of Iowa, Iowa City, Iowa, USA;
[6] Key Laboratory of Tibetan Environment Changes and Land Surface Processes, Institute of Tibetan Plateau Research, Chinese Academy of Sciences, Beijing 100101, China;
[7] State Key Laboratory of Cryospheric Science, Northwest Institute of Eco-Environment and Resources, Chinese Academy of Sciences, Lanzhou 730000, China;
[8] Northeast Institute of Geography and Agroecology, Chinese Academy of Sciences, Changchun 130102, China;
[9] CAS Center for Excellence in Tibetan Plateau Earth Sciences, China.

Corresponding author: Jun Zhu (junzhu@nuist.edu.cn) & Xiangao Xia (xxa@mail.iap.ac.cn)

Abstract:

The long-term temporal-spatial variations of aerosol optical properties in Tibetan Plateau (TP) and the potential long-range transport from surrounding areas to TP were analyzed in this work, by using multiple years of sunphotometer measurements (CE318) at five stations in TP, satellite aerosol productions from Moderate Resolution Imaging Spectroradiometer (MODIS) and Cloud-Aerosol Lidar with Orthogonal Polarization (CALIOP), back-trajectory analysis from the Hybrid Single-Particle Lagrangian Integrated Trajectory (HYSPLIT) and model simulation of the Goddard Earth Observing System (GEOS)-Chem chemistry transport model. The results from ground-based observations show that the annual aerosol optical depth (AOD) at most TP sites increased in the past decades with trends of 0.001±0.003/year at Lhasa, 0.013±0.003/year at Mt_WLG, 0.002±0.002/year at NAM_CO, and 0.000±0.002/year at QOMS_CAS. The increasing trend is also found for the aerosol Extinction Ångstrom exponent (EAE) at most sites, except for Mt_WLG sites with an obvious decreasing trend. Spatially, the AOD observed from MODIS shows negative trends in the northwest edge closed to the Taklimakan Desert and east of the Qaidam Basin and slightly positive trends in most of the other area of TP. Different aerosol types and sources contribute to the polluted day (with CE318 AOD at 440nm > 0.4) in the five sites of TP: dust dominant in Lhasa, Mt_WLG and Muztagh with sources from the Taklimakan Desert but fine aerosol pollution dominant at NAM_CO and QOMS_CAS with the transport from South Asia. A case of aerosol pollution at Lhasa,

https://doi.org/10.5194/acp-2019-444
Preprint. Discussion started: 12 June 2019

Atmospheric Chemistry and Physics Discussions

NAM_CO and QOMS_CAS during 28 April – 3 May 2016 reveals that the smoke aerosols in South Asia were lifted up to 10km and transported to TP, while the dust from Taklimakan Desert could climb the north slope of TP and then be transported to center TP. The long-range transport thereby seriously impact aerosol loading over the TP.

Keywords: Aerosol optical depth, Tibetan Plateau, aerosol pollution, long-range transport

https://doi.org/10.5194/acp-2019-444
Preprint. Discussion started: 12 June 2019

Atmospheric Chemistry and Physics Discussions

1. Introduction

The heavy haze occurred in past years in China was largely attributed to the atmospheric aerosol (Zhang et al., 2015). Besides, atmospheric aerosols can affect the climate through the interactions between aerosol-radiation and between aerosol-cloud (Takemura et al., 2005;Li et al., 2017), while the cloud and its precipitation are also in connection with the large scale atmospheric circulations (Yang et al., 2010;Yang et al., 2017a). However, the uncertainty of the aerosol climate effect is still high, which is mostly due to the highly spatiotemporal variability of aerosol. Therefore, the study of the aerosol physical and chemical properties over different regions is very essential. Ground-based measurements can offer more accuracy data of aerosol properties, while large scale observation of aerosol optical and physical properties needs satellite remote-sensing method(Li et al., 2015;Li et al., 2018;Xing et al., 2017). Thus, long-term detection of aerosols from both of the ground and satellite platforms is absolutely necessary to improve understanding of the climate effects of aerosol (Kaufman et al., 2002).

The Tibetan Plateau (TP), is the largest elevated plateau in East Asia and considered as one of the most pristine terrestrial regions, alongside the Arctic and Antarctic. However, in the past two decades, TP has been surrounded by the unpreceded growing emissions of Asian air pollutants from the various sources. Consequently, some researches have demonstrated that the aerosols transported from its around areas (South Asia and Taklimakan Desert) have polluted the TP (Huang et al., 2007;Xia et al., 2011;Kopacz et al., 2011;Lu et al., 2012;Liu et al., 2015). Lau et al. (2006) has suggested that increased absorbing aerosols (dust and black carbon) over TP may create a positive tropospheric temperature anomaly over TP and adjacent region to the south, causing the advance and enhancement of the Indian summer monsoon. While attempts were made to reveal the linkages between the climate change (such as glaciers and monsoon) and the air pollutant around TP (mainly absorbing carbonaceous materials) (Qian et al., 2011;Wang et al., 2016;Xie et al., 1999;Lee et al., 2013), the quantitative effect of the TP aerosol on climate variability remains largely unknown, and there is an urgent need to fully understand the aerosol characteristics over TP.

Past studies analyzing the aerosol variation in TP used ground-based observations and satellite products (Cong et al., 2007;Zhang et al., 2012;Wan et al., 2015;Tobo et al., 2007;Zhao et al., 2013;Liu et al., 2008;Du et al., 2015), but many of these studies focused on the single station or short-term variation due to the difficulties to take the sufficient number of observations in challenging weather conditions over the remote plateau. Consequently, our work here is to focus on the long-term temporal-spatial variations of the aerosol optical properties over multiple stations over TP and the aerosol properties and sources during the aerosol pollution events in TP based on multiple years of five ground-based sunphotometer observations and the MODIS aerosol optical depth product in TP. In addition, we will also combine the observation and models to study the aerosol transport process over TP, thereby helping to reduce the uncertainties in estimate of aerosol radiative forcing and aerosol sources.

In this paper, section 2 describes the observation site, data and method are. The results of temporal-spatial variations of aerosol properties over TP is shown in Section 3. The analysis of aerosol pollution and an aerosol transport case are presented in section 4 and 5, respectively. The conclusions are in section 6.

https://doi.org/10.5194/acp-2019-444
Preprint. Discussion started: 12 June 2019

Atmospheric Chemistry and Physics Discussions

2. Site, data and Methodology

2.1 site

In this study, five sites in TP equipped with the sun and sky scanning radiometer (CE318) were used (Figure 1). Table 1 shows the station location and description. Lhasa station is the only urban site where can suffer from the local anthropogenic emissions. As for the other four sites, local anthropogenic emissions are extremely rare due to few signs of human habitation. However, Mt_WLG is in the northeast of TP where is situated at the dust transport path from the maximal desert of China (the Taklimakan Desert). Muztagh_Ata site is located in the northwest corner of TP and beside the Central Asian Deserty Areas and Taklimakan Desert. NAM_CO is located in the central Tibetan Plateau, 220 km away from Lhasa. QOMS_CAS is located at the northern slope of Mt. Qomolangma on the border of Tibet and Nepal. Therefore, these five sites can stand for the spatial feature of the TP.

2.2 Data

2.2.1 CE318 aerosol optical properties

The column-integrated aerosol properties over the five TP sites are derived from CE318 measurements. Table 1 has showed the observation period. The CE318 instrument measures direct solar spectral radiation and the angular distribution of sky radiance. These spectral radiances can be used to retrieval aerosol optical parameters (such as aerosol optical depth (AOD)) based on Beer Law, aerosol microphysical properties (such as volume size distribution) and its radiative forcing features through radiation transfer theory. AOD, Extinction Ångstrom exponent (EAE), and aerosol volume size distribution (dV(r)/dlnr) are used in this work. Eck et al. (1999) showed the uncertainty of AOD was about 0.01 to 0.02. EAE is calculated from AOD at 440 and 870 nm. The errors of retrieval dV(r)/dlnr are less than 10% in the maxima of the dV(r)/dlnr and may increase up to 35% for the minimum values of dV(r)/dlnr within the radius range between 0.1 μm and 7 μm; for the edges of retrieval size, the errors increase apparently, which does not significantly affect the derivation of the main feature of dV(r)/dlnr (Dubovik et al., 2002).

2.2.2 The MODIS AOD product

Moderate Resolution Imaging Spectroradiometer (MODIS) instrument is a multi-spectral sensor with a wide spectral range from 0.4 to 14.4μm in 36 wavelength bands, onboard the Terra (morning descending directions) and Aqua (afternoon ascending directions) satellites in polar orbit, respectively. It's broad swath of 2330km permits retrieval aerosol products to cover the global word with 1-2 days. In this study, both Terra and Aqua MODIS Collection 6 Deep-Blue/Dark-Target combined AOD at 550nm product with 10km spatial resolution (MODIS_AOD) (Levy et al., 2013) from 2006 to 2017 are used. The MODIS_AOD has been widely validated in the global or regional areas (Bilal et al., 2018;Ma et al., 2016;Sayer et al., 2014). The root-mean-square error of MODIS_AOD was about 0.13 and the percentage of MODIS_AOD within the expected error was larger than 71% at the Kunming site which around the TP (Zhu et al., 2016).

2.2.3 The CALIOP profile data

The Cloud-Aerosol Lidar with Orthogonal Polarization (CALIOP), the primary instrument on board of CALIPSO satellite, is a near-nadir viewing two wavelength (532 nm and 1064 nm)

https://doi.org/10.5194/acp-2019-444
Preprint. Discussion started: 12 June 2019

Atmospheric Chemistry and Physics Discussions

polarization-sensitive lidar which performs global vertical profiles measurements of aerosols and clouds (Winker et al., 2010). It provides three primary calibrated and geolocated products of profiles: total attenuated backscatter at 532 nm and 1064 nm and the perpendicular polarization component at 532 nm. The data used in this study include the attenuated backscattering coefficient profiles from level 1B and vertical feature mask data products of aerosol subtype from level 2 products under 15 km altitude, which are downloaded from the Langley Atmospheric Science Data Center (ASDC).

2.3 Methodology

The ground-based CE318 observations and MODIS AOD products are analyzed to show the temporal-spatial variations of aerosol properties in TP.

The CE318 observed AOD larger than 0.4 at each site is considered as the aerosol pollution over TP. The back trajectories are used for aerosol source analysis in TP. Back trajectories for the aerosol pollution study are calculated by using the Hybrid Single-Particle Lagrangian Integrated Trajectory (HYSPLIT) model which is driven by the one degree horizontal resolution archived meteorological fields with (Draxler and Hess, 1998). 72-hour back trajectories ending at the five site at 10 m above ground level at 12 UTC on the day of aerosol pollution (AOD at 440 nm >0.4) are used to identify the air mass sources.

Case study is based on ground CE318 observation over Lhasa, NAM_CO and QOMS_CAS. By combing HYSPLIT back trajectories, MODIS and CALIOP products, and the Goddard Earth Observing System (GEOS)-Chem chemistry transport model, the aerosol source and type during the case is analyzed. The GEOS-Chem chemical transport model version 11-01 coupled with online radiative transfer calculations (RRTMG) at 0.5° × 0.667° horizontal resolution over the East Asia domain is used to simulate aerosol variation during the case period (Bey et al., 2001;Wang et al., 2004). The default configuration schemes respectively for advection, transport, convection, deposition, and the emissions are used for the model simulation of full chemistry.

3. Temporal-spatial variations of aerosol properties

3.1 Temporal variation of aerosol properties

Annual variation of CE318 AOD and EAE over TP at the four sites, i.e. Lhasa, Mt_WLG, NAM_CO, and QOMS_CAS are shown in Figure 2. The data of the CE318 observation at Muztagh_Ata site are available only during 2010, thus the annual variation at this site is not shown here. The annual AOD shows increased trends of 0.001±0.003/year at Lhasa, 0.013±0.003/year at Mt_WLG, and 0.002±0.002/year at NAM_CO during CE318 observed period. Mt_WLG site shows the most obvious increase of AOD during 2009-2013. These indicate the increase of aerosol loading in the three sites. The long-term annual variation of AOD at QOMS_CAS is very small (0.000±0.002/year), but there still exists short-term annual variation (decreased from 2010 to 2013 and increased from 2013 to 2016). The annual trends of EAEs show more evident than the AOD in these four site. Most sites show the increased tendency of annual–averaged EAE, except for Mt_WLG sites with a large decreasing trend of -0.318±0.081/year. This showed the size of aerosol at Mt_WLG sites increased, while the size of aerosol decreased in other three sites. Combing the AOD and EAE, the positive trend of AOD with the positive trend of EAE in the long term at most sites over TP indicates the addition of fine mode aerosol mainly from the anthropogenic impact. But

https://doi.org/10.5194/acp-2019-444
Preprint. Discussion started: 12 June 2019

Atmospheric Chemistry and Physics Discussions

in the short term, the increase of annual averaged AOD is often with the decrease of EAE over TP, which suggests the addition of coarse mode aerosol during the CE318 observation.

Monthly and seasonal statistics of CE318 AOD and EAE are shown in Figure 3 and Table 2, respectively. Distinct monthly and seasonal variability of the AOD and EAE over the five sites can be found. The monthly mean AOD shows the highest value in April at Lhasa (0.19), NAM_CO (0.09) and QOMS_CAS (0.10) sites, while highest in June (0.20) at Mt_WLG. The monthly mean AOD rapidly increases from January to April, then slightly decreases to December at Lhasa, NAM_CO and QOMS_CAS sites. However, the AOD at Mt_WLG shows almost symmetry form from January to December. The monthly variation of EAE is different from the AOD at each site. The highest monthly EAE occurs in September at Lhasa (1.15), October at Mt_WLG (1.15) and January at NAM_CO (0.93) and QOMS_CAS (0.17) sites. The EAE at QOMS_CAS also shows a high value of 0.17 in April, which may be caused by the smoke aerosol transported from South Asia during this period. The monthly mean EAE decreases firstly from January to March, then increases to September at Lhasa. Monthly EAE at NAM_CO also decreases from January to March, but does not increase apparently in the followed months. The EAE at Mt_WLG shows a decrease from January to May and then increases obviously from May to October. Lhasa, NAM_CO, and QOMS_CAS sites are near and located in the south of TP. Thus, the variations of aerosol properties in these three sites are similar. The Mt_WLG is located in the northeast of TP, which is different from the south sites. The Muztagh_Alt is in the northwest of TP and nearest the Taklimakan desert, which cause the high AOD there (a few observed data may be another reason). Combing the AOD and EAE, the high AOD is often accompanied by the low EAE at Lhasa, Mt_WLG and NAM_CO, indicating these sites suffered from the coarse aerosol such as dust (Huang et al., 2007;Liu et al., 2015;Zhang et al., 2001). However, QOMS_CAS sites show the high AOD and high EAE at April, which is related to the smoke aerosols transported from South Asia.

A distinct seasonal AOD and EAE variation can be found over TP sites. AOD mean values in fall (SON) and winter (DJF) are lower at all sites except Muztagh. Muztagh_Ata shows high AOD in both observed seasons. Except Muztagh, the maximal seasonal AOD is observed in spring (MAM) (Lhasa, NAM_CO, and QOMS_CAS) or in summer (JJA) (Mt_WLG). The minimal seasonal EAE occurred in spring (Lhasa, NAM_CO and Mt_WLG) or summer (QOMS_CAS), while maximal EAE is mostly observed in fall (Lhasa and Mt_WLG) and winter (NAM_CO and QOMS_CAS). These indicate frequently dust events over TP in spring period at Lhasa, NAM_CO and Mt_WLG. Mt_WLG is situated at the dust transport path from the Taklimakan Desert, which causes the high AOD observed in spring and summer in this site.

The seasonal size distributions of the five sites in Figure 4 also demonstrate that coarse mode aerosol is dominant at the five TP sites in almost all seasons, which is different from the eastern pollution regions of China with fine mode aerosol dominant, such as Yangtze River Delta (Zhuang et al., 2018). These explained the relative lower EAE in the five sites (annual EAE<1.0), which was lower than the inland urban and suburban sites in China (Xin et al., 2007), for the example of Beijing, Nanjing(Zhuang et al., 2017), Kunming (Zhu et al., 2016), Chengdu (Che et al., 2015). What's more, spring is the season with high volume concentration of coarse mode aerosol. Among the five sites, the southernmost sites, QOMS_CAS, showed the highest mean EAE and the size distribution was

https://doi.org/10.5194/acp-2019-444
Preprint. Discussion started: 12 June 2019

Atmospheric Chemistry and Physics Discussions

distinct bimodal, especially in spring. This was also because of the frequently biomass burning activity in India and Nepal which can transport the fine aerosol to the QOMS_CAS site.

3.2 Spatial variation of aerosol properties

The spatial distribution of MODIS annual AOD is show in Figure 5. The MODIS AOD is agreement with the AOD observed by CE318 at the five TP sites. The northwest area around the Taklimakan desert and the north part lied in the transport path of Taklimakan Desert dust showed the high AOD (>0.25) in past decades. Besides, the southern edge performed slightly high AOD (0.2-0.25) influenced by the aerosol transport from South Asia. There exists some little area with high AOD (~0.2) in the center of TP and the southeast region is shown of low AOD (~1.0), which may be attributed to the aerosol transport and surface feature such as vegetable cover since there are few inhabitants. The seasonal departure of MODIS AOD (Figure 6) shows that high positive AOD departure often appears in spring, especially for the northwest edge, north area and south edge of TP, which was result from the aerosol transport from the frequent dust events at Taklimakan and fire activities in South Asia in spring.

A linear regression trend analysis of MODIS annual AOD at 550nm over TP from 2006 to 2017 was conducted using the least square method. The spatial distribution of annual trends in MODIS AOD during 2006-2017 is illustrated in Figure 7. There are no statistically significant trends in most areas during 2006-2007. The AOD performed negative trends in the northwest edge closed to Taklimakan Desert and the east of the Qaidam Basin and slightly positive trends in most of the other area. The AOD descending area is mainly the place near the desert or lied in the transport path of desert dust. This descending trend may be related to the significant reduction in dust emissions caused by the decline in wind speed in recent years (Yang et al., 2017b). The positive trend in other most area may be due to the rapid increase in human activities, such as the expend of tourism to TP and the biomass burning in South Asia.

The seasonal trends of MODIS AOD at 550 nm over TP during 2006-2017 is present in Figure 8. The spring showed the most obvious of the decline in AOD (~ 0.02/year) in the north edges and northeast part of TP during 2006 - 2017, which also suggested the reduction of dust impact from the Taklimakan Desert as the trend of annual MODIS AOD (seen in Figure 7). In summer, the positive trend of AOD over TP was relative apparent and most higher sporadic positive values of ~0.01 occurred in central and south part of TP. Summer is the tourist season over TP and the tourism has developed in past decades, which may be one of the reasons of the higher positive trend in summer in TP. The apparent positive trends in autumn and winter were relative less than summer and most positive trends were located at the northern TP. The reason of this phenomenon needs to be explored.

4. Aerosol pollution at Tibetan plateau

The mean AOD in TP is normally low for its little trace of human habitation and high altitude. However, some high AODs with larger than 0.4 had been observed at the five site in TP by CE318. The aerosol properties and source of the high AOD (>0.4) in TP need to be studied.

Figure 9 shows the AOD with values larger than 0.4 versus EAE observed by CE318 at the five sites in TP. Except the Lhasa and Mt_WLG sites, almost all values of AOD are less than 1.0,

https://doi.org/10.5194/acp-2019-444
Preprint. Discussion started: 12 June 2019

Atmospheric Chemistry and Physics Discussions

which reflects the relative clear environment over TP. The EAE shows two centers of ~0.1 and ~1.5. The low EAE (~0.1) center is related to the dust events which can cause higher concentration of coarse particles in the atmosphere. Besides, most values of low EAE (<0.5) part are less than 0.2 (only few of EAE between 0.2-0.5 is observed at Lhasa and Mt_WLG), indicating the pure dust type is more than the polluted dust type in TP according to Eck et al. (2010). The high EAE center in ~1.5 indicates the mainly small sub-micron radius particles which is attributed to the anthropologic emissions. There can be found that the values of EAE >1.0 part at NAM_CO and QOMS_CAS are generally higher than Lhasa and Mt_WLG sites. According to the past studies, the EAE of urban/industry aerosol is generally high than the biomass burning aerosol (Giles et al., 2012;Eck et al., 2010), which may cause the higher EAE at NAM_CO and QOMS_CAS (more biomass burning aerosol) than Lhasa and Mt_WLG (more urban/industry aerosol). On the other hand, the values with in the middle of 0.5-1.0 is rare, indicating the less mix of nature and human sources. The percentage of EAE bins to the number of CE318 AOD>0.4 is distinct from each other sites (Table 3). The percentage of EAE <0.5 is high than that EAE>1.0 at Lhasa, Mt_WLG and Muztagh_Ata, indicating more nature dust pollution than the anthropologic pollution at these three sites. However, more high EAE (>1.0) is observed than EAE<0.5 at NAM_CO and QOMS_CAS sites, suggesting that anthropologic pollution is more than nature dust pollution at these two sites.

Figure 10 shows the aerosol size distribution binned by AOD at the five sites in TP. The volume concentration of coarse mode particles increases more apparently than fine mode at Lhasa, Mt_WLG and Muztagh sites when the values of AOD increase. However, the size distribution at NAM_CO and QOMS_CAS shows the dominant increasing of fine mode aerosol. These indicate of the different aerosol type pollution in these five sites: dust dominant in Lhasa, Mt_WLG and Muztagh and fine mode aerosol (mainly biomass burning aerosol) pollution dominant at NAM_CO and QOMS_CAS.

The dominant aerosol pollution type showed the obvious distinction in the five sites at TP, then where is the distinct aerosol pollution source at each site? We use the HYSPLIT back-trajectory model and MODIS AOD on the aerosol pollution day (CE318 AOD >0.4) to show the aerosol source on pollution day at each site. Figure 11 is the 72 hour back-trajectories ended at the five site (10 m above ground level) in TP overlaid by the mean MODIS AOD at 550 nm on the aerosol pollution day observed by ground-based CE318 (CE318 AOD >0.4). The CE318 instruments have observed 78, 20, 2, 15, 14 days with instantaneous AOD at 440 nm > 0.4 at Lhasa, Mt_WLG, Muztagh_Ata, NAM_CO and QOMS_CAS, respectively. The aerosol pollution days at Lhasa, Mt_WLG, and Muztagh_Ata observed by CE318 are often with low EAE (black trajectories). The airflows ended the Lhasa site on polluted days are mainly from northwest and southwest. The MODIS AOD around Lhasa in the area of back-trajectories with CE318 EAE <0.5 passing does not show significant high values, especially in the Taklimakan Desert, which indicates the dust pollution at Lhasa is mainly from local or around dust events rather than transport from Taklimakan Desert. The Mt_WLG shows that air mass on the pollution days comes from west and east and the way of back trajectories is with high MODIS AOD. The high values of MODIS AOD has shown two transport paths of dust aerosol to Mt_WLG: one is through the Qaidam Basin and another is through northeast edge of TP. The two polluted days observed by CE318 at Muztagh_Ata shows the east airflows originated from Taklimakan Desert. The direction of the back-trajectories of EAE<0.5 ended at NAM_CO is similar

https://doi.org/10.5194/acp-2019-444
Preprint. Discussion started: 12 June 2019

Atmospheric Chemistry and Physics Discussions

to Lhasa, while the south air flows with high EAE (red trajectories) is originated from Nepal where frequent biomass burning happened and caused the high MODIS AOD values. The trajectories ended at QOMS_CAS and the high MODIS AOD of its passing has shown the transport of smoke aerosol from South Asia to this site.

5. Case study of long-range transport to TP

A specific case of aerosol pollution during 27 April - 3 May 2016 is analyzed further. This case is selected based on the observations of CE318 instrument. During 28 April -1 May, the AOD observed by CE318 at Lhasa, NAM_CO, QOMS_CAS sites showed up the values larger than 0.4, which value reached up more than 3 times of the mean values of AOD of each site (0.11 at Lhasa, 0.05 at NAM_CO and QOMS_CAS). This is indicative of the aerosol pollution at the three sites. Then, how about the aerosol properties of this period and where the polluted aerosol come from?

Figure 12 shows the daily AOD and EAE during 27 April – 03 May at the three sites. The mean values of AOD from CE318 Sun photometer were 0.45, 0.38, 0.23 at Lhasa, NAM_CO and QOMS_CAS, respectively. These even reached to 4 times of the annual mean AOD at each site. The mean EAEs were 0.98, 1.22, 1.44 at Lhasa, NAM_CO and QOMS_CAS, respectively, which was relative higher than the annual averages and suggested the fine aerosol entrance. There were AOD peaks at the three sites during 27 April – 03 May. Lhasa showed the increase of AOD from 0.30 on 27 April to 0.51 on 28 April, and kept high AOD to 0.54 on 1 May, after that decreased to 0.34 on 2 May. NAM_CO also showed the increase of AOD at the first two days, but decreased after 29 April. QOMS_CAM showed a slight increase of AOD from 27 April to 40 April, which was later than other two sites. Combing the EAE on these days, fine mode aerosol was brought in Lhasa and NAM_CO during 27-29 April, and then coarse aerosol occurred on 30 April, and even became the dominant aerosol in the following several days. The fine aerosol at the QOMS_CAM site kept an extra day than the two sites and then coarse aerosol increased.

The GEOS-Chem model simulation also supported above results. Figure 13 shows the comparison between the GEOS-Chem model simulated AOD (0.5° × 0.667°) and CE318 observed AOD and the ratios of the model simulated aerosol type (dust, both organic carbon (OC) and black carbon (BC) aerosol) to the total AOD during this case period at the three sites. The evaluation results showed that the model underestimated the daily AOD at the three sites during the period. However, the model AOD was relatively high correlated with the CE318 AOD, with the correlation coefficient (R) of 0.61 at Lhasa, 0.89 at NAM_CO and 0.86 at QOMS_CAS. Thus, AOD variation trend from the model simulation was in good agreement with that measured by the CE318 instruments during these days. During the first 4 days (27 April to 30 April), the ratios of different aerosol to total AOD showed that the sum of OC and BC aerosol was higher than dust aerosol at all the three sites. Besides, the sum of OC and BC at Lhasa and QOMS_CAS was higher NAM_CO. These indicated that the smoke aerosol affected the three sites more severely than dust during the first 4 days and Lhasa and QOMS_CAS sites were nearer to smoke source than NAM_CO. After 30 April, the sum of BC and OC was decreased while dust increased, and the increase of dust at the three sites was NAM_CO > Lhasa > QOMS_CAS. Therefore, the major aerosol source was changed and NAM_CO was closer to dust source after 40 April. This phenomenon had continued to 2 May at NAM_CO and Lhasa, and 1 May at QOMS_CAS. At the last one or two days, the dust decreased

https://doi.org/10.5194/acp-2019-444
Preprint. Discussion started: 12 June 2019

Atmospheric Chemistry and Physics Discussions

while smoke increased obviously, which could cause the mixture of this two aerosols.

Then, how is the spatial aerosol loading around TP and vertical feature of aerosol transported to TP? Figure 14 shows MODIS C6 AOD at 550nm and 72h back trajectories at Lhasa (the first row), CALIOP-derived vertical profile of total attenuated backscatter at 532 nm (the second row), and the vertical feature mask of aerosol (the third row) on April 28, May 1, and May 3 during this period. The MODIS AOD showed high values in south (South Asia) and north (Taklimakan Desert) on the three days. High values in South Asia was caused by biomass burning, while high AOD in Taklimakan Desert was resulted from the dust. The value and area of high AOD in South Asia and Taklimakan Desert on May 1 and May 3 were higher and larger than that on April 28. The back–trajectories ended at Lhasa on the three days were different. On 28 April, air flows were originated from the southwest (South Asia region). However, air masses on 1 and 3 May were from the northwest (Taklimakan Desert).

The CALIPSO ground track across TP and through South Asia and Taklimakan Desert were chose to show the aerosol transport to the TP sites. On 28 April, the level 1 attenuated backscatter at 532nm derived from CALIOP (the second row) showed apparent aerosol layers in South area (Bhutan and northeast India) and this aerosol lay even lifted to ~10km altitude in the sky over TP along the south slop of TP. On 1 May, the CALIOP attenuated backscatter not only showed the deep aerosol layers in south of TP but also showed stronger aerosol layers in the north of TP (Taklimakan Desert area). Besides, the north aerosol layers also climbed to air over the TP, but not high as the south aerosol layer. On 3 May, there were also aerosol layers on south and north of TP and they both were transported to TP overhead, but the aerosol loading over TP was lower than that on 28 April and 1 May (the values of attenuated backscatter on 3 May was lower), which caused the AOD observed by CE318 at the three TP sites (Figure 12) on this day was lower than 28 April and 1 May.

The vertical feature mask of aerosol from CALIOP (the third row) shows the aerosol type on the three days. On 28 April, the aerosol layer in the north (about 35°N) and above TP was mainly the smoke aerosol and even higher than 10km. The back trajectories ended at Lhasa also showed the southern airflow brought the smoke aerosol from South Asia to the center of TP. On 1 May, the aerosol layer in south slop of TP was also the smoke aerosol, while the aerosol layers in the north of TP and TP overhead were almost all dust aerosol, which may be the result of the lower EAE at Lhasa and NAM_CO than that at QOMS_CAM (Figure 12). After two days mixing, the aerosol type above the central TP and south TP on 3 May has been occupied by the polluted dust aerosol, and the EAE at NAM_CO and QOMS_CAM also showed a little increase on 3 May. These agree with aerosol simulation of GEOS-Chem. The observations and model simulation illustrate a scene: firstly, the smoke aerosol in South Asia was lifted up to 10km, contaminated the TP sites and transported to center of TP; then the dust from Taklimakan Desert could climb the north slope of TP and be transported to TP; the dust and smoke aerosol over the TP were mixed at last. This case of aerosol pollution shows the smoke in South Asia and Dust in Taklimakan Desert could be transported to center TP and they both even can cause the mixed aerosol pollution above the TP. The past cases studies of aerosol transport to TP are almost individual dust or smoke aerosol, while this case of aerosol pollution over TP has shown the mixing pollution during the last two days.

https://doi.org/10.5194/acp-2019-444
Preprint. Discussion started: 12 June 2019

Atmospheric Chemistry and Physics Discussions

6. Conclusion

The long-term temporal-spatial variations of aerosol optical properties and aerosol long-range transport impact over TP were analyzed by using a combination of ground and satellite remote sensing aerosol products as well as model simulations. The major conclusions are drawn as follows:

(1) The annual AOD at most TP sites showed increasing trends during the past decade: 0.001±0.003/year at Lhasa, 0.013±0.003/year at Mt_WLG, 0.002±0.002/year at NAM_CO, and 0.000±0.002/year at QOMS_CAS. Most sites showed the increased tendency of annual–averaged EAE, except for Mt_WLG sites with a large decreasing trend of -0.318/year. Spatially, the AOD showed negative trends in the northwest edge closed to Taklimakan Desert and the east of Qaidam Basin and slightly positive trends in most of the other area of TP.

(2) The values of EAE with AOD>0.4 at five TP ground stations showed two centers of ~0.1 and ~1.5. The EAE and size distribution during the aerosol polluted day (CE318 AOD at 440 nm > 0.4) at the TP showed the different aerosol type pollution in the five sites: dust dominant in Lhasa, Mt_WLG and Muztagh and fine mode aerosol pollution dominant at NAM_CO and QOMS_CAS. The back-trajectories on polluted days indicated the dust aerosol mainly come from the Taklimakan Desert and fine mode aerosol was mainly transported from South Asia.

(3) A case of smoke followed by dust pollution at Lhasa, NAM_CO and QOMS_CAS during 28 April – 3 May 2016 was analyzed: firstly, the smoke aerosol in South Asia was lifted up to 10km and transported to the center of TP, then the dust from Taklimakan Desert could climb the north slope of TP and be transported to TP, the dust and smoke aerosol over the TP were mixed at last.

There are some limitations in this study. First, ground-based remote sensing and MODIS AOD product may have missed conditions interfered with clouds. Second, only half year of observations at Muztagh_Ata station may not be sufficient to fully reveal pollution days in the northwest TP region, which will affect the statistics to some extent. More long-term in situ observations are needed in TP. However, due to the remoteness and challenging weather conditions over the plateau, maintaining in situ observation stations over TP in long term is very difficult. The numerical model simulation is more practically feasible to study the aerosol properties over TP, but the model accuracy is far from being ideal over TP. Thus, long-term numerical model simulation coupling with satellite observation and intensive short-term field campaigns should be used to analyze the aerosol properties over TP in the future.

Data availability:

The four sites (Mt_WLG, Muztagh_Ata, NAM_CO and QOMS_CAS) data are available from AERONET website (https://aeronet.gsfc.nasa.gov/). The dataset of Lhasa used in the study can be requested by contacting the corresponding author. The MODIS aerosol products are available from http://ladsweb.nascom.nasa.gov. The HYSPLIT model and meteorological fields' data can be from https://www.arl.noaa.gov/hysplit/. The CALIPSO data are from https://eosweb.larc.nasa.gov. GEOS-Chem model code and share data can be obtained from http://wiki.seas.harvard.edu/geos-chem.

Competing interests.

The authors declare that they have no conflict of interest.

https://doi.org/10.5194/acp-2019-444
Preprint. Discussion started: 12 June 2019

Atmospheric Chemistry and Physics Discussions

Author contribution:

All authors help to shapethe ideas and review this manuscript. JZ, XX and HC designed, and wrote the manuscript; JZ, XX, HC, JW help to analyze the data; HC, XZ, SK and ZC carried out the sunphotometer observations; JW, ZC, SK, TZ, XY, and YZ provided constructive comments on this study.

Acknowledgments

This research was supported by the National Science Fund for Distinguished Young Scholars (41825011), the National Key R & D Program Pilot Projects of China (2016YFA0601901 and 2016YFC0203304), the National Natural Science Foundation of China (41761144056), the Strategic Priority Research Program of Chinese Academy of Sciences (XDA20040500), the Natural Science Foundation of Jiangsu Province (BK20170943), the Open fund by the Key Laboratory for Middle Atmosphere and Global Environment Observation (LAGEO) / Institute of Atmospheric Physics, and LAC/CMA (2018B02).

https://doi.org/10.5194/acp-2019-444
Preprint. Discussion started: 12 June 2019

Atmospheric Chemistry and Physics Discussions

References

Bey, I., Jacob, D. J., Yantosca, R. M., Logan, J. A., Field, B. D., Fiore, A. M., Li, Q., Liu, H. Y., Mickley, L. J., and Schultz, M. G.: Global modeling of tropospheric chemistry with assimilated meteorology: Model description and evaluation, Journal of Geophysical Research: Atmospheres, 106, 23073-23095, https://doi.org/10.1029/2001jd000807, 2001.

Bilal, M., Nazeer, M., Qiu, Z., Ding, X., and Wei, J.: Global Validation of MODIS C6 and C6.1 Merged Aerosol Products over Diverse Vegetated Surfaces, Remote Sens-Basel, 10, 475, https://doi.org/10.3390/rs10030475, 2018.

Che, H., Zhang, X. Y., Xia, X., Goloub, P., Holben, B., Zhao, H., Wang, Y., Zhang, X. C., Wang, H., Blarel, L., Damiri, B., Zhang, R., Deng, X., Ma, Y., Wang, T., Geng, F., Qi, B., Zhu, J., Yu, J., Chen, Q., and Shi, G.: Ground-based aerosol climatology of China: aerosol optical depths from the China Aerosol Remote Sensing Network (CARSNET) 2002–2013, Atmospheric Chemistry and Physics, 15, 7619-7652, https://doi.org/10.5194/acp-15-7619-2015, 2015.

Cong, Z., Kang, S., Liu, X., and Wang, G.: Elemental composition of aerosol in the Nam Co region, Tibetan Plateau, during summer monsoon season, Atmospheric Environment, 41, 1180-1187, https://doi.org/10.1016/j.atmosenv.2006.09.046, 2007.

Draxler, R. R., and Hess, G. D.: An overview of the HYSPLIT-4 Modelling system for trajectories, dispersion and deposition, Australian Meteorological Magazine, 47, 295-308, 1998.

Du, W., Sun, Y. L., Xu, Y. S., Jiang, Q., Wang, Q. Q., Yang, W., Wang, F., Bai, Z. P., Zhao, X. D., and Yang, Y. C.: Chemical characterization of submicron aerosol and particle growth events at a national background site (3295 m a.s.l.) on the Tibetan Plateau, Atmospheric Chemistry and Physics, 15, 10811-10824, https://doi.org/10.5194/acp-15-10811-2015, 2015.

Dubovik, O., Holben, B., Eck, T. F., Smirnov, A., Kaufman, Y. J., King, M. D., Tanré, D., and Slutsker, I.: Variability of Absorption and Optical Properties of Key Aerosol Types Observed in Worldwide Locations, Journal of the Atmospheric Sciences, 59, 590-608, https://doi.org/10.1175/1520-0469(2002)059<0590:voaaop>2.0.co;2, 2002.

Eck, T. F., Holben, B. N., Reid, J. S., Dubovik, O., Smirnov, A., O'Neill, N. T., Slutsker, I., and Kinne, S.: wavelength dependence of the optical depth of biomass burning, urban, and desert dust aerosols, Journal of Geophysical Research, 104, 31,333-331,349, 1999.

Eck, T. F., Holben, B. N., Sinyuk, A., Pinker, R. T., Goloub, P., Chen, H., Chatenet, B., Li, Z., Singh, R. P., Tripathi, S. N., Reid, J. S., Giles, D. M., Dubovik, O., O'Neill, N. T., Smirnov, A., Wang, P., and Xia, X.: Climatological aspects of the optical properties of fine/coarse mode aerosol mixtures, J Geophys Res-Atmos, 115, https://doi.org/10.1029/2010jd014002, 2010.

Giles, D. M., Holben, B. N., Eck, T. F., Sinyuk, A., Smirnov, A., Slutsker, I., Dickerson, R. R., Thompson, A. M., and Schafer, J. S.: An analysis of AERONET aerosol absorption properties and classifications representative of aerosol source regions, J Geophys Res-Atmos, 117, 127-135, https://doi.org/10.1029/2012JD018127, 2012.

Huang, J., Minnis, P., Yi, Y., Tang, Q., Wang, X., Hu, Y., Liu, Z., Ayers, K., Trepte, C., and Winker, D.: Summer dust aerosols detected from CALIPSO over the Tibetan Plateau, Geophys Res Lett, 34, 529-538, https://doi.org/10.1029/2007gl029938, 2007.

Kaufman, Y. J., Tanre, D., and Boucher, O.: A satellite view of aerosols in the climate system, Nature, 419, 215-223, https://doi.org/10.1038/Nature01091, 2002.

Kopacz, M., Mauzerall, D., Wang, J., Leibensperger, E., Henze, D., and Singh, K.: Origin and radiative forcing of black carbon transported to the Himalayas and Tibetan Plateau,

https://doi.org/10.5194/acp-2019-444
Preprint. Discussion started: 12 June 2019

Atmospheric Chemistry and Physics, 11, 2837-2852, https://doi.org/10.5194/acp-11-2837-2011, 2011.

Lau, K. M., Kim, M. K., and Kim, K. M.: Asian summer monsoon anomalies induced by aerosol direct forcing: the role of the Tibetan Plateau, Clim Dynam, 26, 855-864, https://doi.org/10.1007/s00382-006-0114-z, 2006.

Lee, W.-S., Bhawar, R. L., Kim, M.-K., and Sang, J.: Study of aerosol effect on accelerated snow melting over the Tibetan Plateau during boreal spring, Atmospheric environment, 75, 113-122, https://doi.org/10.1016/j.atmosenv.2013.04.004, 2013.

Levy, R. C., Mattoo, S., Munchak, L. A., Remer, L. A., Sayer, A. M., Patadia, F., and Hsu, N. C.: The Collection 6 MODIS aerosol products over land and ocean, Atmos Meas Tech, 6, 2989-3034, https://doi.org/10.5194/amt-6-2989-2013, 2013.

Li, J., Huang, J., Stamnes, K., Wang, T., Lv, Q., and Jin, H.: A global survey of cloud overlap based on CALIPSO and CloudSat measurements, Atmospheric Chemistry and Physics, 15, 519-536, https://doi.org/10.5194/acp-15-519-2015, 2015.

Li, J., Lv, Q., Zhang, M., Wang, T., Kawamoto, K., Chen, S., and Zhang, B.: Effects of atmospheric dynamics and aerosols on the fraction of supercooled water clouds, Atmospheric Chemistry & Physics, 17, 1847-1863, https://doi.org/10.5194/acp-17-1847-2017, 2017.

Li, J., Jian, B., Huang, J., Hu, Y., Zhao, C., Kawamoto, K., Liao, S., and Wu, M.: Long-term variation of cloud droplet number concentrations from space-based Lidar, Remote Sensing of Environment, 213, 144-161, https://doi.org/10.1016/j.rse.2018.05.011, 2018.

Liu, Y., Sato, Y., Jia, R., Xie, Y., Huang, J., and Nakajima, T.: Modeling study on the transport of summer dust and anthropogenic aerosols over the Tibetan Plateau, Atmospheric Chemistry and Physics, 15, 12581-12594, https://doi.org/10.5194/acp-15-12581-2015, 2015.

Liu, Z., Liu, D., Huang, J., Vaughan, M., Uno, I., Sugimoto, N., Kittaka, C., Trepte, C., Wang, Z., Hostetler, C., and Winker, D.: Airborne dust distributions over the Tibetan Plateau and surrounding areas derived from the first year of CALIPSO lidar observations, Atmospheric Chemistry and Physics, 8, 5045-5060, https://doi.org/10.5194/acp-8-5045-2008, 2008.

Lu, Z., Streets, D. G., Zhang, Q., and Wang, S.: A novel back-trajectory analysis of the origin of black carbon transported to the Himalayas and Tibetan Plateau during 1996-2010, Geophys Res Lett, 39, n/a-n/a, https://doi.org/10.1029/2011gl049903, 2012.

Ma, Y., Li, Z., Li, Z., Xie, Y., Fu, Q., Li, D., Zhang, Y., Xu, H., and Li, K.: Validation of MODIS Aerosol Optical Depth Retrieval over Mountains in Central China Based on a Sun-Sky Radiometer Site of SONET, Remote Sens-Basel, 8, 111, https://doi.org/10.3390/rs8020111, 2016.

Pöschl, U.: Atmospheric aerosols: composition, transformation, climate and health effects, Angewandte Chemie International Edition, 44, 7520-7540, https://doi.org/10.1002/anie.200501122, 2006.

Qian, Y., Flanner, M. G., Leung, L. R., and Wang, W.: Sensitivity studies on the impacts of Tibetan Plateau snowpack pollution on the Asian hydrological cycle and monsoon climate, Atmospheric Chemistry and Physics, 11, 1929-1948, https://doi.org/10.5194/acp-11-1929-2011, 2011.

Sayer, A. M., Munchak, L. A., Hsu, N. C., Levy, R. C., Bettenhausen, C., and Jeong, M. J.: MODIS Collection 6 aerosol products: Comparison between Aqua's e-Deep Blue, Dark Target, and "merged" data sets, and usage recommendations, Journal of Geophysical Research:

https://doi.org/10.5194/acp-2019-444
Preprint. Discussion started: 12 June 2019

Atmospheric Chemistry and Physics Discussions

Atmospheres, 119, 13,965-913,989, https://doi.org/10.1002/2014jd022453, 2014.

Takemura, T., Nozawa, T., Emori, S., Nakajima, T. Y., and Nakajima, T.: Simulation of climate response to aerosol direct and indirect effects with aerosol transport-radiation model, Journal of Geophysical Research, 110, -, https://doi.org/10.1029/2004jd005029, 2005.

Tobo, Y., Iwasaka, Y., Shi, G.-Y., Kim, Y.-S., Ohashi, T., Tamura, K., and Zhang, D.: Balloon-borne observations of high aerosol concentrations near the summertime tropopause over the Tibetan Plateau, Atmospheric research, 84, 233-241, https://doi.org/10.1016/j.atmosres.2006.08.003, 2007.

Wan, X., Kang, S., Wang, Y., Xin, J., Liu, B., Guo, Y., Wen, T., Zhang, G., and Cong, Z.: Size distribution of carbonaceous aerosols at a high-altitude site on the central Tibetan Plateau (Nam Co Station, 4730ma.s.l.), Atmospheric Research, 153, 155-164, https://doi.org/10.1016/j.atmosres.2014.08.008, 2015.

Wang, X., Ren, J., Gong, P., Wang, C., Xue, Y., Yao, T., and Lohmann, R.: Spatial distribution of the persistent organic pollutants across the Tibetan Plateau and its linkage with the climate systems: a 5-year air monitoring study, Atmospheric Chemistry and Physics, 16, 6901-6911, https://doi.org/10.5194/acp-16-6901-2016, 2016.

Wang, Y. X., McElroy, M. B., Jacob, D. J., and Yantosca, R. M.: A nested grid formulation for chemical transport over Asia: Applications to CO, Journal of Geophysical Research: Atmospheres, 109, n/a-n/a, https://doi.org/10.1029/2004jd005237, 2004.

Winker, D. M., Pelon, J., Coakley, J. A., Ackerman, S. A., Charlson, R. J., Colarco, P. R., Flamant, P., Fu, Q., Hoff, R. M., Kittaka, C., Kubar, T. L., Le Treut, H., McCormick, M. P., Megie, G., Poole, L., Powell, K., Trepte, C., Vaughan, M. A., and Wielicki, B. A.: THE CALIPSO MISSION A Global 3D View of Aerosols and Clouds, B Am Meteorol Soc, 91, 1211-1229, https://doi.org/10.1175/2010bams3009.1, 2010.

Wu, G. X., Liu, Y. M., Wang, T. M., Wan, R. J., Liu, X., Li, W. P., Wang, Z. Z., Zhang, Q., Duan, A. M., and Liang, X. Y.: The influence of mechanical and thermal forcing by the Tibetan Plateau on Asian climate, Journal of Hydrometeorology, 8, 770-789, https://doi.org/10.1175/Jhm609.1, 2007.

Xia, X. G., Zong, X. M., Cong, Z. Y., Chen, H. B., Kang, S. C., and Wang, P. C.: Baseline continental aerosol over the central Tibetan plateau and a case study of aerosol transport from South Asia, Atmospheric Environment, 45, 7370-7378, https://doi.org/10.1016/j.atmosenv.2011.07.067, 2011.

Xie, S. C., Yao, T. D., Kang, S. C., Duan, K. Q., Xu, B. Q., and Thompson, L. G.: Climatic and environmental implications from organic matter in Dasuopu glacier in Xixiabangma in Qinghai-Tibetan Plateau (SCI), Science in China, 42, 383-391, 1999.

Xin, J. Y., Wang, Y. S., Li, Z. Q., Wang, P. C., Hao, W. M., Nordgren, B. L., Wang, S. G., Liu, G. R., Wang, L. L., Wen, T. X., Sun, Y., and Hu, B.: Aerosol optical depth (AOD) and Angstrom exponent of aerosols observed by the Chinese Sun Hazemeter Network from August 2004 to September 2005, J Geophys Res-Atmos, 112, 1703-1711, https://doi.org/10.1029/2006jd007075, 2007.

Xing, C., Liu, C., Wang, S., Chan, K. L., Gao, Y., Huang, X., Su, W., Zhang, C., Dong, Y., Fan, G., Zhang, T., Chen, Z., Hu, Q., Su, H., Xie, Z., and Liu, J.: Observations of the vertical distributions of summertime atmospheric pollutants and the corresponding ozone production in Shanghai, China, Atmos. Chem. Phys., 17, 14275-14289,

https://doi.org/10.5194/acp-2019-444
Preprint. Discussion started: 12 June 2019

https://doi.org/10.5194/acp-17-14275-2017, 2017.

Yang, K., Wu, H., Qin, J., Lin, C., Tang, W., and Chen, Y.: Recent climate changes over the Tibetan Plateau and their impacts on energy and water cycle: A review, Global Planet Change, 112, 79-91, https://doi.org/10.1016/j.gloplacha.2013.12.001, 2014.

Yang, R., Wang, J., Zhang, T., and He, S.: Change in the relationship between the Australian summer monsoon circulation and boreal summer precipitation over Central China in the late 1990s, Meteorology and Atmospheric Physics, 131, 105-113, https://doi.org/10.1007/s00703-017-0556-3, 2017a.

Yang, R. W., Tao, Y., and Cao, J.: A Mechanism for the Interannual Variation of the Early Summer East Asia-Pacific Teleconnection Wave Train, Acta Meteorol Sin, 24, 452-458, 2010.

Yang, Y., Russell, L. M., Lou, S., Liao, H., Guo, J., Liu, Y., Singh, B., and Ghan, S. J.: Dust-wind interactions can intensify aerosol pollution over eastern China, Nat Commun, 8, 15333, https://doi.org/10.1038/ncomms15333, 2017b.

Zhang, B., Wang, Y., and Hao, J.: Simulating aerosol–radiation–cloud feedbacks on meteorology and air quality over eastern China under severe haze conditionsin winter, Atmospheric Chemistry and Physics, 15, 2387-2404, https://doi.org/10.5194/acp-15-2387-2015, 2015.

Zhang, N., Cao, J., Ho, K., and He, Y.: Chemical characterization of aerosol collected at Mt. Yulong in wintertime on the southeastern Tibetan Plateau, Atmospheric Research, 107, 76-85, https://doi.org/10.1016/j.atmosres.2011.12.012, 2012.

Zhang, X. Y., Arimoto, R., Cao, J. J., An, Z. S., and Wang, D.: Atmospheric dust aerosol over the Tibetan Plateau, Journal of Geophysical Research: Atmospheres, 106, 18471-18476, https://doi.org/10.1029/2000jd900672, 2001.

Zhao, Z., Cao, J., Shen, Z., Xu, B., Zhu, C., Chen, L. W. A., Su, X., Liu, S., Han, Y., Wang, G., and Ho, K.: Aerosol particles at a high-altitude site on the Southeast Tibetan Plateau, China: Implications for pollution transport from South Asia, Journal of Geophysical Research: Atmospheres, 118, 11,360-311,375, https://doi.org/10.1002/jgrd.50599, 2013.

Zhu, J., Xia, X., Che, H., Wang, J., Zhang, J., and Duan, Y.: Study of aerosol optical properties at Kunming in southwest China and long-range transport of biomass burning aerosols from North Burma, Atmospheric Research, 169, 237-247, https://doi.org/10.1016/j.atmosres.2015.10.012, 2016.

Zhuang, B. L., Wang, T. J., Liu, J., Li, S., Xie, M., Han, Y., Chen, P. L., Hu, Q. D., Yang, X. Q., Fu, C. B., and Zhu, J. L.: The surface aerosol optical properties in the urban area of Nanjing, west Yangtze River Delta, China, Atmospheric Chemistry and Physics, 17, 1143-1160, https://doi.org/10.5194/acp-17-1143-2017, 2017.

Zhuang, B. L., Wang, T. J., Liu, J. N. E., Che, H. Z., Han, Y., Fu, Y., Li, S., Xie, M., Li, M. M., Chen, P. L., Chen, H. M., Yang, X. Q., and Sun, J. N.: The optical properties, physical properties and direct radiative forcing of urban columnar aerosols in the Yangtze River Delta, China, Atmospheric Chemistry and Physics, 18, 1419-1436, https://doi.org/10.5194/acp-18-1419-2018, 2018.

https://doi.org/10.5194/acp-2019-444
Preprint. Discussion started: 12 June 2019

Atmospheric Chemistry and Physics Discussions

Figure captions

Figure 1. Topography of Tibetan Plateau (TP) and the five CE318 stations located in TP (Lhasa, Mt_WLG, Mutztagh_Ata, NAM_CO, and QOMS_CAS).

Figure 2. Annual average and the trends of aerosol optical depth (AOD) and Extinction Ångstrom exponent (EAE) at four sites located in Tibetan Plateau.

Figure 3. Box plots of monthly AOD and EAE at the five sites located in Tibetan Plateau, i.e. Lhasa, Mt_WLG, Muztagh_Alt, NAM_CO, and QOMS_CAS. In each box, the central red-line is the median and the lower and upper limits are the first and the third quartiles, respectively. The lines extending vertically from the box indicate the spread of the distribution with the length being 1.5 times the difference between the first and the third quartiles. The asterisk symbols indicate the geometric means.

Figure 4. Seasonal variation of aerosol size distribution at the five sites located in Tibetan Plateau.

Figure 5. Spatial distribution of MODIS C6 AOD at 550nm over Tibetan Plateau (only the altitude > 3000m) during 2006-2017. The circle with color filled is the CE318 observation AOD averages at TP sites.

Figure 6. The seasonal departure of MODIS AOD over TP (altitude >3000m).

Figure 7. Trend of MODIS AOD at 550nm during 2006-2017.

Figure 8. Trends of MODIS AOD at 550nm during 2006-2017 in each season.

Figure 9. AOD vs EAE (Only CE318 AOD at 440nm > 0.4 is considered) observed by CE318 at the five site Tibetan plateau.

Figure 10. Aerosol size distribution binned by CE318 AOD at the five sites in Tibetan plateau.

Figure 11. Back-trajectories ended at the five site (10 m above ground level) in TP overlaid by the mean MODIS C6 AOD at 550 nm on the aerosol pollution day observed by ground base CE318 (CE318 AOD >0.4). Red stands for EAE >1.0, black is EAE <0.5, and green is for EAE within 0.5-1.0.

Figure 12. CE318 observed daily AOD at 440nm and EAE during April 27, 2016 – May 3, 2016 at Lhasa, NAM_CO and QOMS_CAS.

Figure 13. The GEOS-Chem model simulated daily average AOD vs CE318 observed daily AOD at 550nm and the ratios of dust or organic carbon (OC) and black carbon (BC) aerosol to the total AOD during April 27, 2016 – May 3, 2016 at Lhasa, NAM_CO and QOMS_CAS.

Figure 14. MODIS C6 AOD at 550nm and 72h back trajectories at Lhasa (first row), CALIOP-derived vertical profile of total attenuated backscatter at 532 nm (second row), vertical feature mask of aerosol on April 28, May 1, and May 3, 2016 over the ground track shown in the first row (green line) (third row).

https://doi.org/10.5194/acp-2019-444
Preprint. Discussion started: 12 June 2019

Atmospheric Chemistry and Physics Discussions

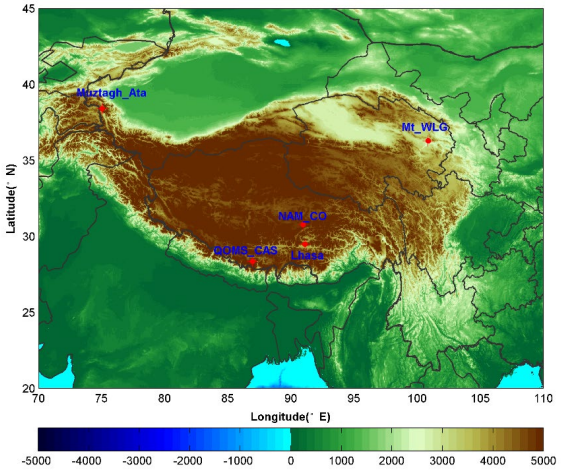

Figure 1. Topography of Tibetan Plateau (TP) and the five CE318 stations located in TP (Lhasa, Mt_WLG, Mutztagh_Ata, NAM_CO, and QOMS_CAS).

https://doi.org/10.5194/acp-2019-444
Preprint. Discussion started: 12 June 2019

Atmospheric Chemistry and Physics Discussions

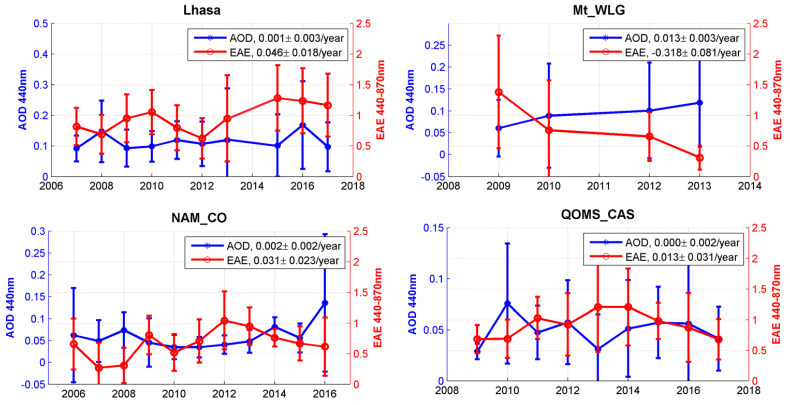

Figure 2. Annual average and the trends of aerosol optical depth (AOD) and Extinction Ångstrom exponent (EAE) at four sites located in Tibetan Plateau.

https://doi.org/10.5194/acp-2019-444
Preprint. Discussion started: 12 June 2019

Atmospheric Chemistry and Physics Discussions

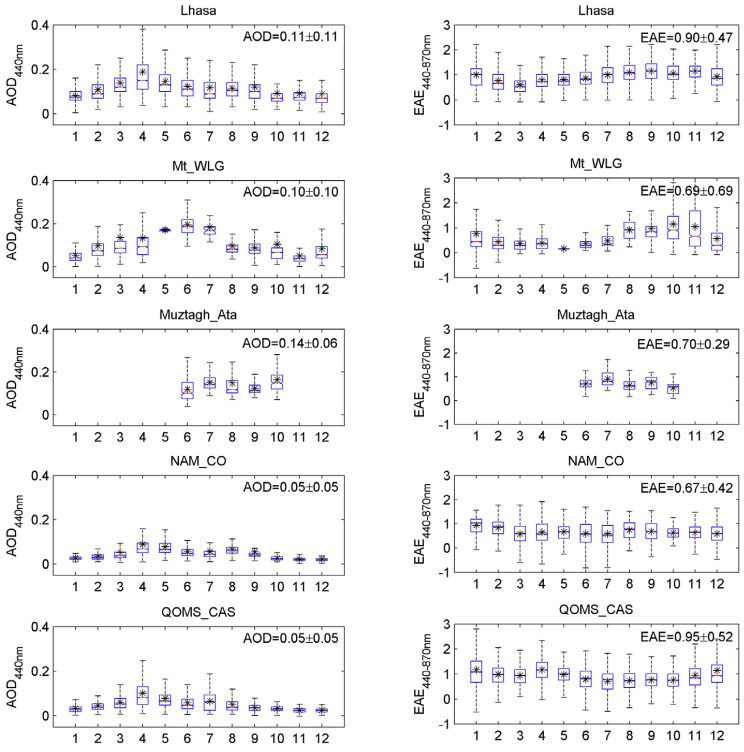

Figure 3. Box plots of monthly AOD and EAE at the five sites located in Tibetan Plateau, i.e. Lhasa, Mt_WLG, Muztagh_Alt, NAM_CO, and QOMS_CAS. In each box, the central red-line is the median and the lower and upper limits are the first and the third quartiles, respectively. The lines extending vertically from the box indicate the spread of the distribution with the length being 1.5 times the difference between the first and the third quartiles. The asterisk symbols indicate the geometric means.

https://doi.org/10.5194/acp-2019-444
Preprint. Discussion started: 12 June 2019

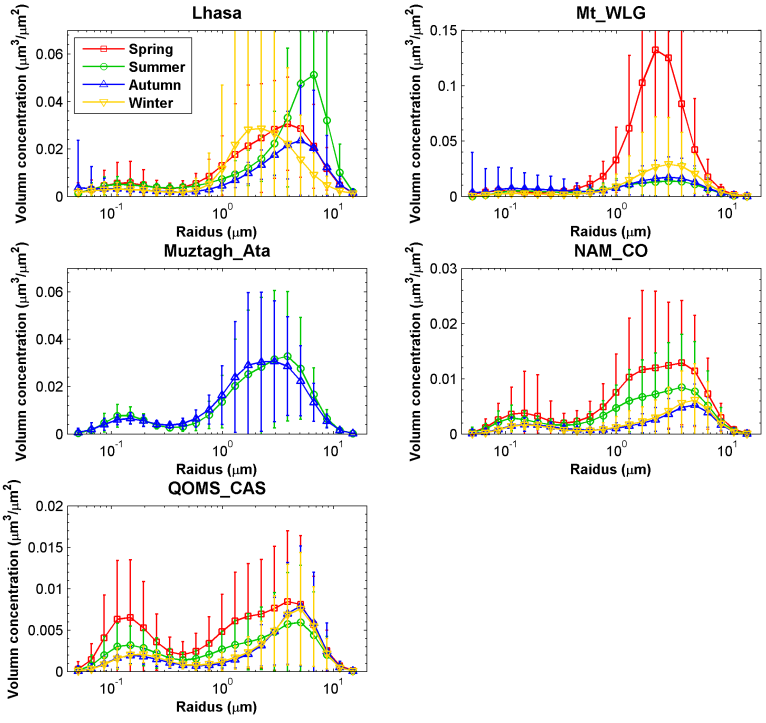

Figure 4. Seasonal variation of aerosol size distribution at the five sites located in Tibetan Plateau.

https://doi.org/10.5194/acp-2019-444
Preprint. Discussion started: 12 June 2019

Atmospheric Chemistry and Physics Discussions

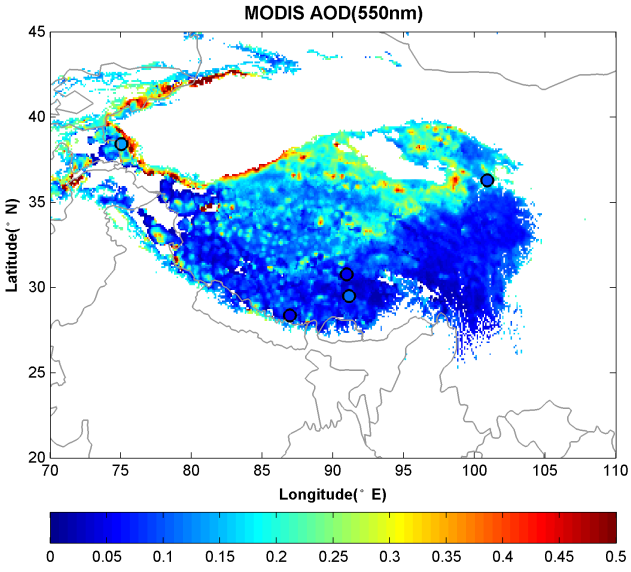

Figure 5. Spatial distribution of MODIS C6 AOD at 550nm over Tibetan Plateau (only the altitude > 3000m) during 2006-2017. The circle with color filled is the CE318 observation AOD averages at TP sites.

https://doi.org/10.5194/acp-2019-444
Preprint. Discussion started: 12 June 2019

Atmospheric Chemistry and Physics Discussions

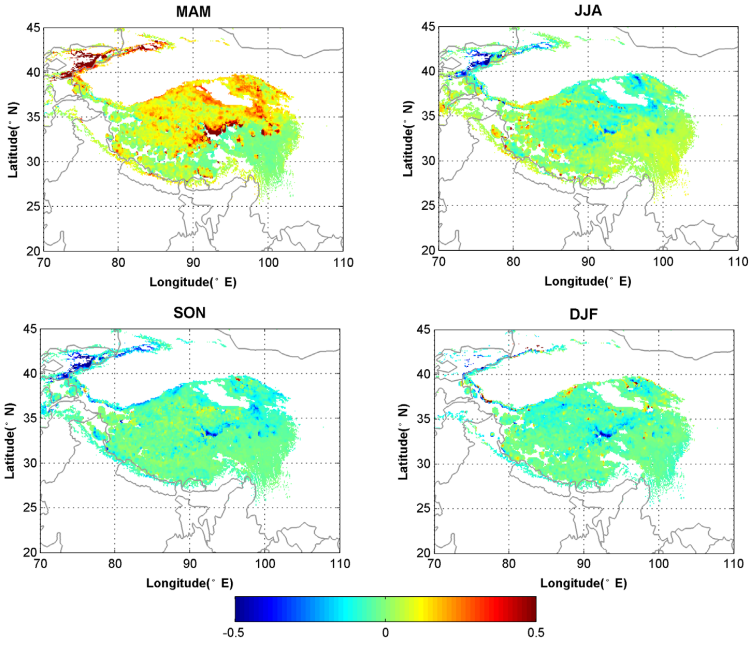

Figure 6. The seasonal departure of MODIS AOD over TP (altitude >3000m).

https://doi.org/10.5194/acp-2019-444
Preprint. Discussion started: 12 June 2019

Atmospheric Chemistry and Physics Discussions

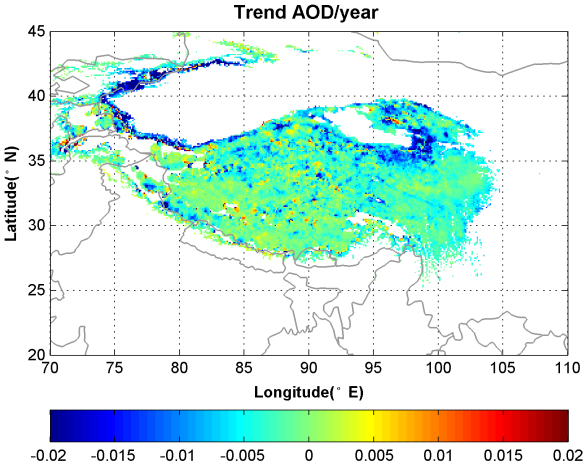

Figure 7. Trend of MODIS AOD at 550nm during 2006-2017.

https://doi.org/10.5194/acp-2019-444
Preprint. Discussion started: 12 June 2019

Atmospheric Chemistry and Physics Discussions

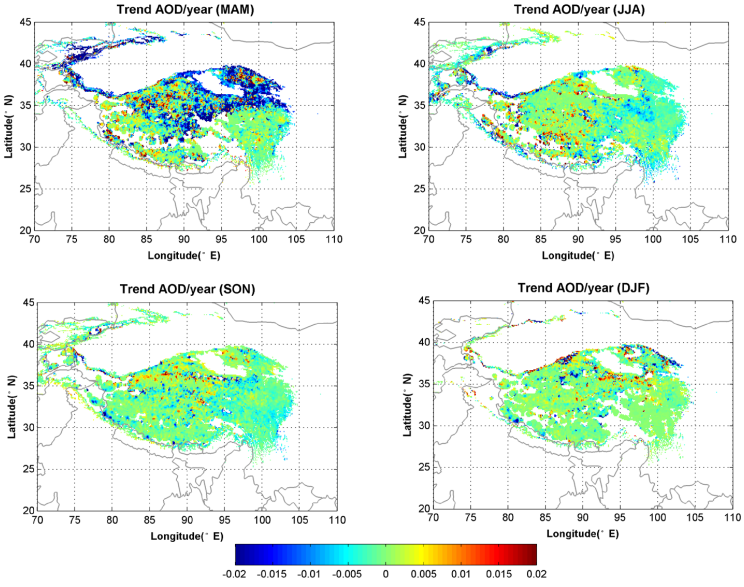

Figure 8. Trends of MODIS AOD at 550nm during 2006-2017 in each season.

https://doi.org/10.5194/acp-2019-444
Preprint. Discussion started: 12 June 2019

Atmospheric Chemistry and Physics Discussions

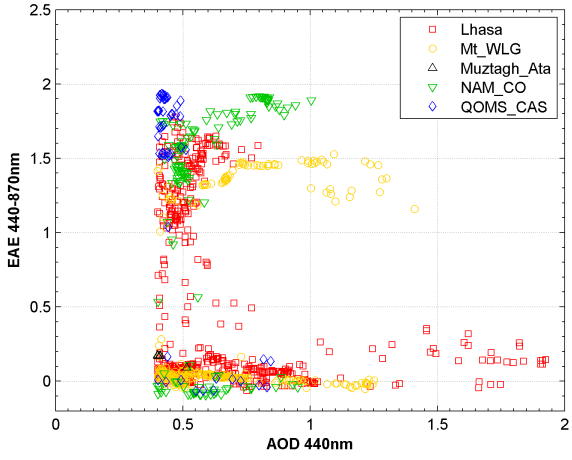

Figure 9. AOD vs EAE (Only CE318 AOD at 440nm > 0.4 is considered) observed by CE318 at the five site Tibetan plateau.

https://doi.org/10.5194/acp-2019-444
Preprint. Discussion started: 12 June 2019

Atmospheric Chemistry and Physics Discussions

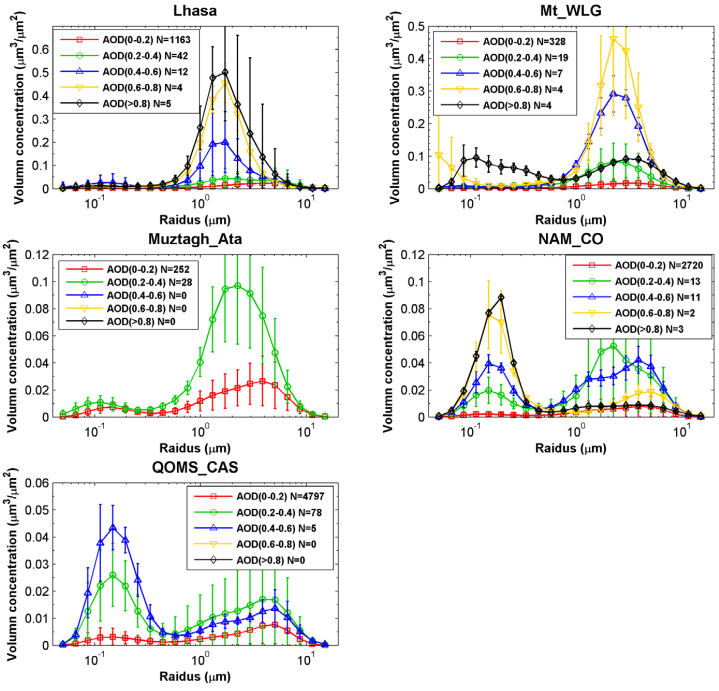

Figure 10. Aerosol size distribution binned by CE318 AOD at the five sites in Tibetan plateau.

https://doi.org/10.5194/acp-2019-444
Preprint. Discussion started: 12 June 2019

Atmospheric Chemistry and Physics Discussions

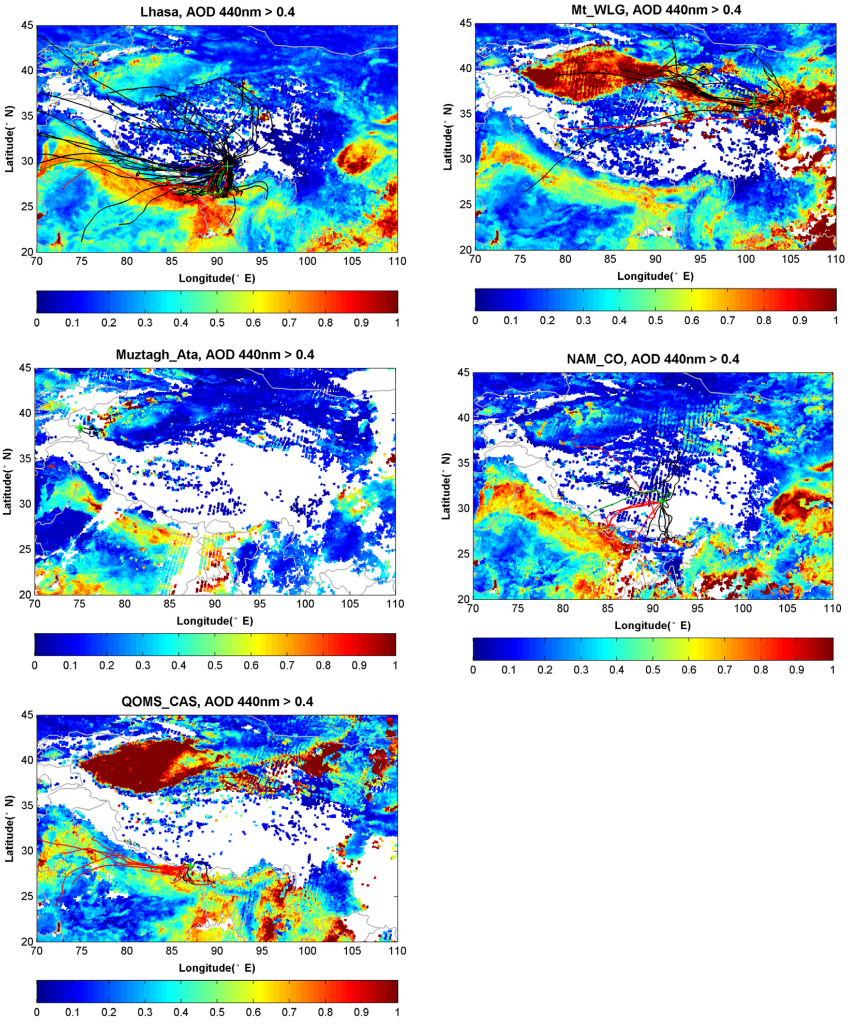

Figure 11. Back-trajectories ended at the five site (10 m above ground level) in TP overlaid by the mean MODIS C6 AOD at 550 nm on the aerosol pollution day observed by ground base CE318 (CE318 AOD >0.4). Red stands for EAE >1.0, black is EAE <0.5, and green is for EAE within 0.5-1.0.

https://doi.org/10.5194/acp-2019-444
Preprint. Discussion started: 12 June 2019

Atmospheric Chemistry and Physics Discussions

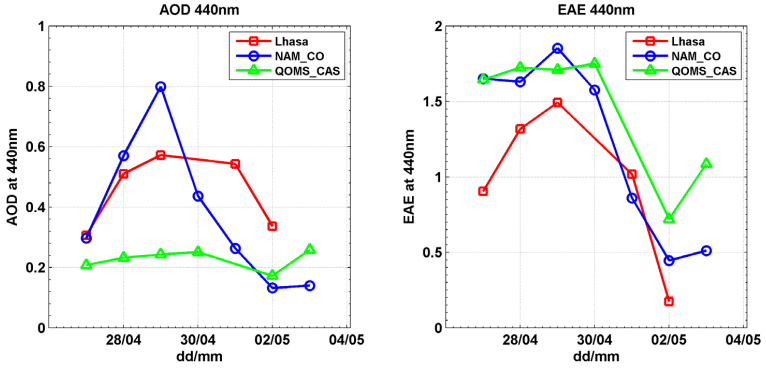

Figure 12. CE318 observed daily AOD at 440nm and EAE during April 27, 2016 – May 3, 2016 at Lhasa, NAM_CO and QOMS_CAS.

https://doi.org/10.5194/acp-2019-444
Preprint. Discussion started: 12 June 2019

Atmospheric Chemistry and Physics Discussions

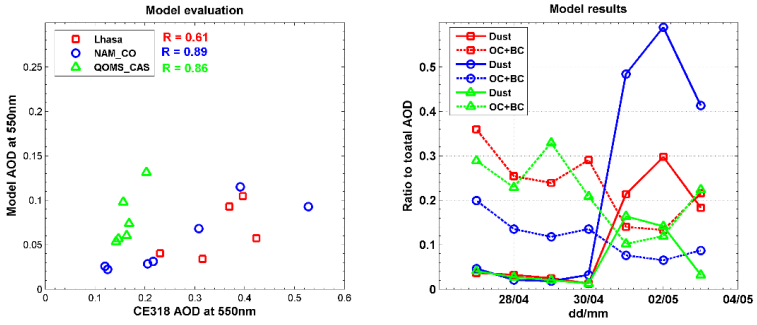

Figure 13. The GEOS-Chem model simulated daily average AOD vs CE318 observed daily AOD at 550nm and the ratios of dust or organic carbon (OC) and black carbon (BC) aerosol to the total AOD during April 27, 2016 – May 3, 2016 at Lhasa, NAM_CO and QOMS_CAS.

https://doi.org/10.5194/acp-2019-444
Preprint. Discussion started: 12 June 2019

Atmospheric Chemistry and Physics Discussions

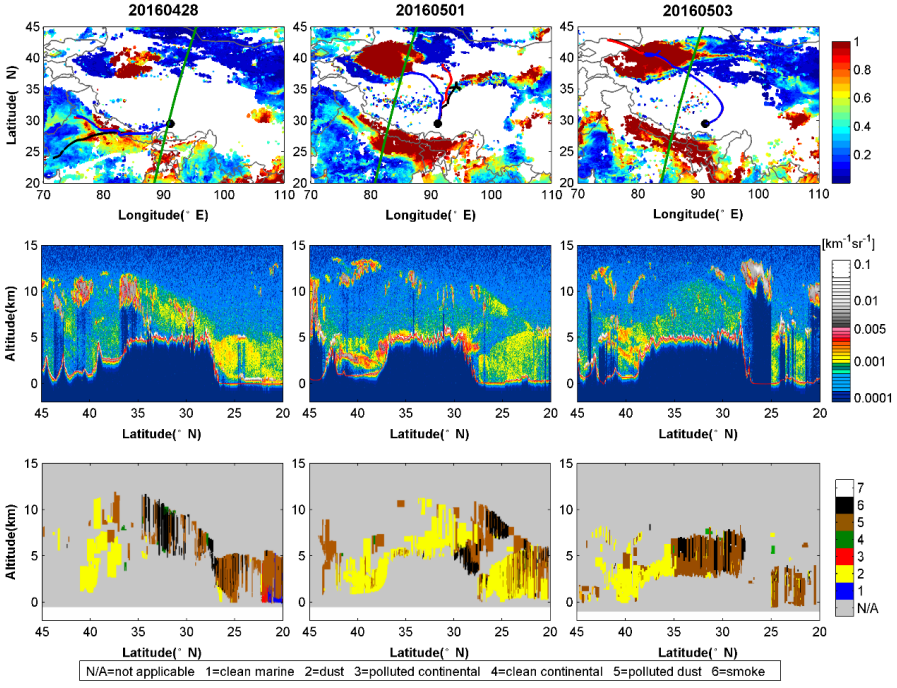

Figure 14. MODIS C6 AOD at 550nm and 72h back trajectories at Lhasa (first row), CALIOP-derived vertical profile of total attenuated backscatter at 532 nm (second row), vertical feature mask of aerosol on April 28, May 1, and May 3, 2016 over the ground track shown in the first row (green line) (third row).

https://doi.org/10.5194/acp-2019-444
Preprint. Discussion started: 12 June 2019

Atmospheric Chemistry and Physics Discussions

Table 1. Site location and description.

Site name	Lat(° N)	Lon(° E)	Site description, observation days and period
Lhasa	29.50	91.13	Urban station over the Tibetan Plateau, 3648m a.s.l., 1554 days, 2007.05~2017.12
Mt_WLG	36.28	100.90	Mountain, 3816 m a.s.l., 314 days, 2009.09~2013.07
Muztagh_Ata	38.41	75.04	Mountain, 3674 m a.s.l., 84 days, 2011.06~2011.10
NAM_CO	30.77	90.96	Mountain, 4740 m a.s.l., 1061 days, 2006.08~2016.08
QOMS_CAS	28.36	86.95	Mountain, 4276 m a.s.l., 1623 days, 2009.10~2017.11

https://doi.org/10.5194/acp-2019-444
Preprint. Discussion started: 12 June 2019

Atmospheric Chemistry and Physics Discussions

Table 2. Seasonal aerosol optical depth (AOD_{440nm}) and extinction Angstrom exponent ($EAE_{440\text{-}870nm}$) at the five sites in TP.

Site	AOD				EAE			
	MAM	JJA	SON	DJF	MAM	JJA	SON	DJF
Lhasa	0.16+0.10	0.12+0.08	0.10+0.18	0.09+0.08	0.72+0.37	0.97+0.40	1.11+0.38	0.91+0.52
Mt_WLG	0.13+0.16	0.14+0.07	0.08+0.11	0.08+0.07	0.37+0.38	0.65+0.40	1.04+0.80	0.58+0.69
Muztagh_Ata	NaN	0.14+0.06	0.14+0.05	NaN	NaN	0.73+0.30	0.64+0.27	NaN
NAM_CO	0.07+0.07	0.06+0.04	0.03+0.05	0.03+0.01	0.63+0.44	0.62+0.45	0.65+0.32	0.78+0.43
QOMS_CAS	0.08+0.06	0.06+0.04	0.03+0.01	0.03+0.02	1.04+0.38	0.76+0.43	0.85+0.51	1.10+0.67

https://doi.org/10.5194/acp-2019-444
Preprint. Discussion started: 12 June 2019

Atmospheric Chemistry and Physics Discussions

Table 3. The percentage of EAE <0.5, 0.5-1.0, and >1.0 for high AOD observations at the five sites.

Site	N of AOD>0.4	% EAE<0.5/N	% 0.5<EAE<1.0/N	% EAE>1.0/N
Lhasa	655	60.6	3.4	36.0
Mt_WLG	290	73.4	0	26.6
Muztagh_Ata	5	100	0	0
NAM_CO	140	27.9	2.8	69.3
QOMS_CAS	59	23.7	0	76.3